Journal Name

COMMUNICATION

Enhancing low-energy absorption band and charge mobility of antiaromatic Ni[II] norcorroles by their substituents effects

Takuya Yoshida,[a] Daisuke Sakamaki,[b] Shu Seki[b] and Hiroshi Shinokubo*[a]

Dissymmetrical substitution of norcorrole enables the preparation of various norcorrole derivatives as air- and moisture-stable species. Intramolecular charge transfer interactions between electron-donating substituents and the norcorrole core in these norcorroles significantly enhanced their low-energy absorption bands, which were forbidden in symmetrical Ni[II] dimesitylnorcorrole.

In recent years, antiaromatic compounds with 4n π-electrons in their planar and cyclic conjugation have been investigated with great interests because they often provide distinctly different properties from those of conventional aromatic compounds. They typically exhibit narrow HOMO–LUMO gaps, reversible redox properties[1] and unique reactivity.[2]

Narrow HOMO–LUMO gaps are particularly attractive to achieve effective near IR (NIR) absorbing organic dyes. Unfortunately, however, antiaromatic compounds inherently exhibit very weak low-energy absorption due to their forbidden HOMO–LUMO transitions. This feature limits their utility as functional dyes for optical application. It is highly desirable to establish a strategy to enhance their low-energy absorbing property. In addition, narrow HOMO–LUMO gaps also allows the design of novel ambipolar semiconductor materials on the basis of 4nπ-electron systems.[3] Nevertheless, systematic fine-tuning of optical and electronic properties of antiaromatic compounds has been a challenging issue because of their inherent instability associated with antiaromatic destabilization.

Norcorrole is one of antiaromatic porphyrinoids,[1bc,4] which was firstly reported by Bröring et al. as an unstable Fe[III] complex.[5] We have previously reported efficient synthesis of Ni[II] dimesitylnorcorrole **1**, which exhibits moderate stability in air and distinct 16π antiaromaticity (Figure 1).[6] With this easily prepared antiaromatic porphyrinoid in hand, we have explored nucleophilic functionalization and hydrogenation of norcorroles, which resulted in modulation of physical properties and antiaromaticity through modification of their pyrrole rings.[7] The reactivity of norcorrole has also been investigated by Li and Chmielewski et al.[8]
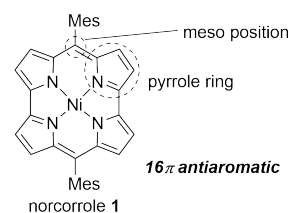

Figure 1. Structure of Ni[II] dimesitylnorcorrole **1**.

The modification of the electronic nature of *meso*-substituents is a conventional but effective approach to modify properties of porphyrinoids. However, the substituent effect at *meso* positions of antiaromatic porphyrinoids has not been explored in detail. In the case of Ni[II] norcorroles, *meso*-aryl groups are limited only to mesityl and phenyl groups. Consequently, we have synthesized Ni[II] norcorroles with various aryl groups and investigated the structural and electronic effects of *meso*-aryl groups of antiaromatic norcorroles. Furthermore, we have demonstrated that intramolecular charge transfer interactions are effective to improve the low-energy absorbing feature of antiaromatic porphyrinoids.

We initially attempted to synthesize norcorroles **2a–2d** with several aryl groups in a symmetrical manner (Scheme 1). Electron-donating 4-dimethylaminophenyl and electron-withdrawing 4-cyanophenyl, 3,5-bistrifluorophenyl and pentafluorophenyl groups were selected as substituents to be introduced at the *meso* positions. Ni[0]-Mediated reductive homo-coupling reactions were performed for α,α'-dibromodipyrrin Ni[II] complexes **3a–3d** to obtain **2a–2d**. However, all attempts to isolate symmetrically substituted norcorroles **2a–2d** resulted in failure due to their instability under ambient conditions.

a. Department of Applied Chemistry, Graduate School of Engineering, Nagoya University, Nagoya 464-8603, Japan. E-mail: hshino@apchem.nagoya-u.ac.jp
b. Department of Molecular Engineering, Graduate School of Engineering, Kyoto University, Nishikyo-ku, Kyoto 615-8510, Japan.
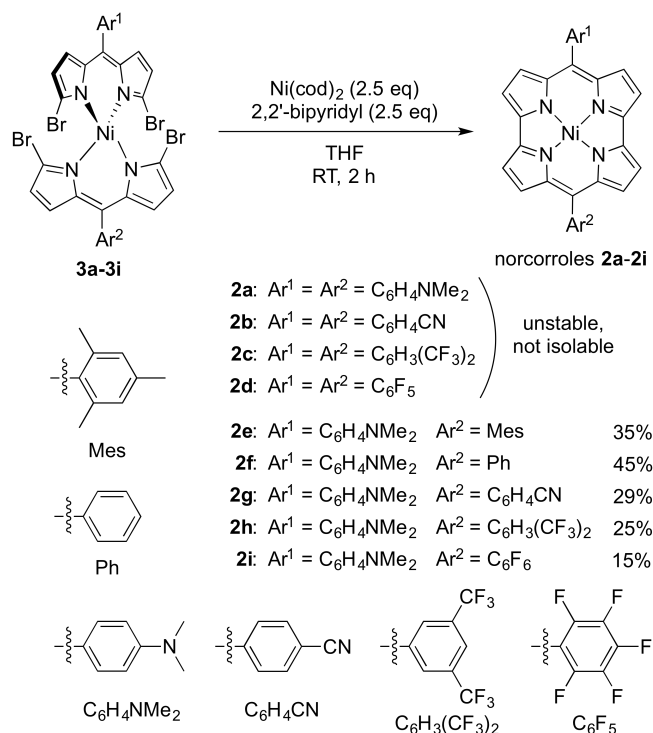
Scheme 1. Structures and synthesis of norcorroles **2a–2i**.

The instability of norcorroles **2a–2d** could be attributed to the change in energy levels of frontier orbitals by substituents. The antiaromatic norcorrole system has inherently high HOMO and low LUMO energy levels, and the former is further destabilized by electron-donating substituents and the latter is further stabilized by electron-withdrawing substituents, thus increasing the instability of norcorroles. On the basis of this consideration, we then introduced two different aryl groups to norcorrole to reduce electron-donating or -withdrawing substituent effects for frontier orbitals. Dissymmetric bisdipyrrin complexes **3e–3i** were prepared by treatment of two different α,α'-dibromodipyrrins with Ni^{II} acetate followed by silica-gel column separation. The homo-coupling reaction of **3e–3i** afforded dissymmetrical norcorroles **2e–2i** with an electron-donating 4-dimethylaminophenyl group on one side (Ar^1), and mesityl, phenyl and three electron-withdrawing substituents on the other side (Ar^2). The stability of **2e–2i** were enhanced as compared with **2a–2d** and **2e–2i** could be isolated in 15–45% yields by silica-gel column purification under ambient conditions. Consequently, the dissymmetric substitution strategy is effective to obtain various antiaromatic and stable norcorroles.

^{1}H NMR spectra of **2e–2i** in CDCl$_3$ exhibited their pyrroles protons in the high-field region (3–2 ppm) due to the paratropic ring current effect, supporting distinct antiaromatic character with 16π-electron systems. Interestingly, the spectrum of **2h** showed concentration dependence, in which the pyrrole protons signals were down-field shifted and significantly broadened at higher concentration of the solution, suggesting its aggregation behaviour (Figure S11).
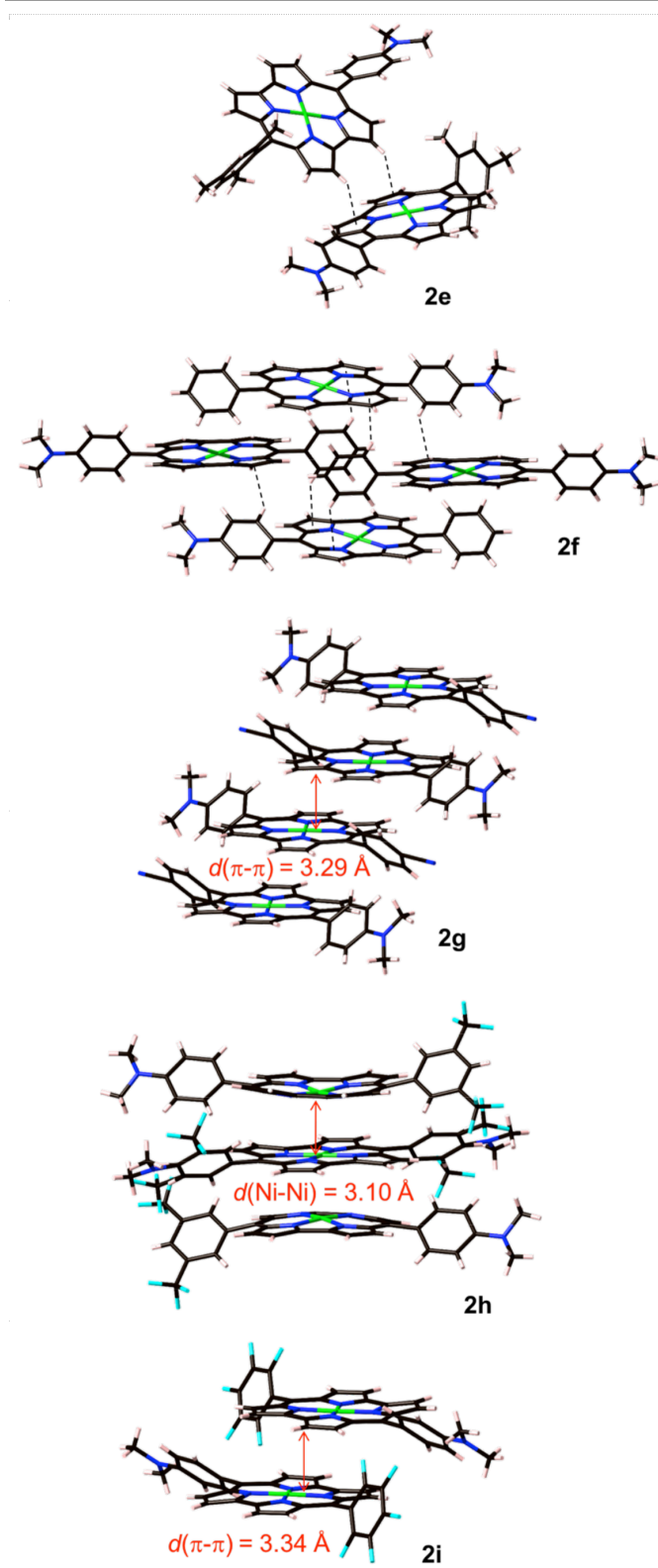
Figure. 2. Packing structures of norcorroles **2e–2i**.

The structures of all dissymmetric norcorroles Ni^{II} complexes **2e–2i** were unambiguously elucidated by X-ray structural analyses. Interestingly, their packing modes varied significantly depending on the subtle change of substituents (Figure 2). In the cases of **2e** and **2f**, the norcorrole

COMMUNICATION

macrocycles are located separately without π-stacking due to dominance of CH–π interactions. On the other hand, π–π stacking between norcorrole planes was observed in the packing structures of **2g**–**2i**, which contain electron-withdrawing groups. Norcorrole planes of **2g** and **2i** show slipped π-stacking with mean plane distances of 3.29 and 3.34 Å, respectively. Interestingly, **2g** formed an infinite π–π stacking structure in the crystal, while packing of **2i** composed of stacked dimeric units. Furthermore, **2h** formed triple-decker stacking structure with a distance of 3.10 Å between Ni atoms, reflecting aggregation behaviour of **2h** observed in the ^{1}H NMR measurement. The two outer norcorroles are slightly distorted but the inner norcorrole maintained planar conformation. A similar triple stacking was also observed in the crystal structure of diphenylnorcorrole Ni^{II}.[7d]
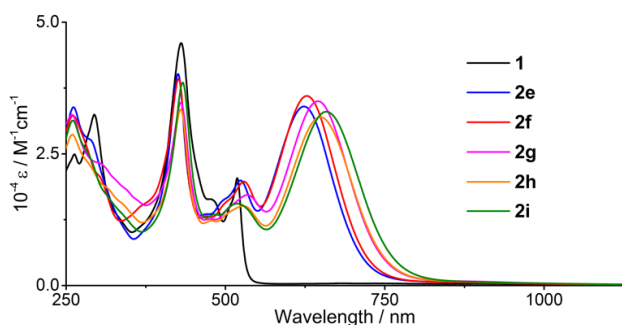

Figure 3. UV-vis-NIR absorption spectra of norcorroles **1** and **2e**–**2i** in CH$_2$Cl$_2$.

UV-vis-NIR absorption spectra of norcorroles **2e**–**2i** and **1** in CH$_2$Cl$_2$ were shown in Figure 3. In contrast to the spectrum of **1**, dissymmetric norcorroles **2e**–**2i** exhibit characteristic intense absorption bands around 650 nm. These bands were further bathochromically shifted by the introduction of electron-withdrawing groups. Meanwhile, the absorption envelope and intensity of **2e**–**2i** are similar to that of **1** except for the bands around 650 nm. These results clearly demonstrated that the use of the substituent effect is effective to enhance the low-energy absorption band of norcorrole.

To investigate the unusual absorption bands of **2e**–**2i**, time-dependent (TD)-density functional theory (DFT) calculations were performed for **2e** and **2i** at the B3LYP/6-31G(d)+SDD level (Figure S19). The result clearly demonstrates that the absorption around 650 nm should be assigned to the transition from HOMO–3 to LUMO, which have significant intermolecular charge transfer character from the electron-donating 4-dimethylaminophenyl group to the norcorrole core (Figure 4, Figure S19 and Table S1). The CT absorption band of **2i** appeared in a lower energy region than that of **2e**. This tendency was well-reproduced by the TD-DFT calculations, which indicated that the red-shifted CT absorption band of **2i** resulted from the lowered LUMO level due to the pentafluorophenyl group. The CT character of this absorption band was also experimentally confirmed by absorption spectra of **2e** measured in various solvents (Figure S15). These spectroscopic and theoretical studies imply that the norcorrole macrocycle behaves as an electron-accepting unit when coupled with electron-donating *meso*-substituents.
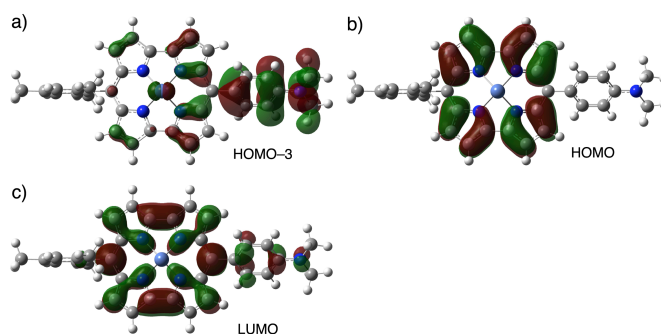

Figurer 4. Selected Kohn–Sham orbitals of **2e** calculated at the B3LYP/6-31G(d)+SDD level. (a) HOMO–3 (b) HOMO and (b) LUMO.

The substituent effect was further evaluated by electrochemistry of dissymmetric norcorroles **2e**–**2i** using cyclic voltammetry measurements (Table 1 and Figure S17). All norcorroles exhibit several reversible oxidation and reduction waves. The first oxidation potentials of all dissymmetric norcorroles **2e**–**2i** exhibited marked cathodic shifts as compared with that of **1** due to the strong electron-donating nature of the 4-dimethylaminophenyl group, while anodic shifts of the first reduction potentials were observed in norcorroles **2g**–**2i** by their electron-withdrawing groups. In addition to electronic properties of substituents, their structural feature also affects the electrochemistry: the first oxidation processes of **2f** and **2h** split into two waves. Norcorroles **2f** and **2h** have Ar^2 groups without *ortho*-substituents, in which dihedral angles with the norcorrole core are smaller than those of **2e** and **2i** (Table S2). The oxidation wave of structurally similar **2g** was not split but broad. These twin waves of **2f** and **2h** should be considered as one-electron oxidation process, which is split by intermolecular interaction during the oxidation. This interpretation was supported by spectroelectrochemical analyses of **2e** and **2h**. The spectral change during the E_{ox1} process of **2e** was almost the same as the change in the case of **2h**, indicating that both oxidation processes are essentially identical (Figure S16, Figure S17). These split resulted in the considerably low oxidation potential of **2f** and **2h** (–0.11 and –0.07 V, respectively).

Table 1. Summary of cyclic voltammetry data for norcorroles **1** and **2e**–**2i**.[a]

Compound	E_{ox2}	E_{ox1}	E_{red1}	E_{red2}	ΔE[b]
1	0.79	0.16	–0.92	–1.70	1.08
2e	0.53	0.05	–0.95	–1.67	1.00
2f	0.63	0.03, –0.11	–0.90	–1.58	0.79
2g	0.63	0.02	–0.85	–1.45	0.87
2h	0.67	0.14, –0.07	–0.81	–1.45	0.74
2i	0.59	0.08	–0.77	–1.46	0.85

[a] Solvent: CH$_2$Cl$_2$, electrolyte: Bu$_4$NPF$_6$, working electrode: glassy carbon, counter electrode: Pt, reference electrode: Ag/AgClO$_4$, scan rate: 0.1 V s^{-1}. The potentials (V) versus the value for the ferrocene/ferrocenium cation couple are shown. [b] ΔE = E_{ox1} – E_{red1}.

The charge carrier conductivities of **2e**–**2i** were evaluated using flash-photolysis time-resolved microwave conductivity (FP-TRMC) technique,[9] since a difference of intermolecular interactions significantly affect conductivity of materials.

Microcrystalline samples of **2e**, **2f, 2h** and **2i** were used for measurement, but a similar sample of **2g** could not be obtained because of its low solubility. The maximum transient conductivities of ($\phi\Sigma\mu$) **2e**–**2i** were summarized in Figure 5 and Figure S18. Norcorroles **2g**–**2i** with π–π stacking structures in their crystals exhibited substantially larger conductivities than **2e** and **2f**, which have none of such interactions (Figure 2). The relatively lower $\phi\Sigma\mu$ value of **2g** than those of **2h** and **2i** would be attributed to its lower crystallinity of the powder sample of **2g**. The result suggests that existence of π–π stacking between norcorrole units should be important to attain higher $\phi\Sigma\mu$ values.
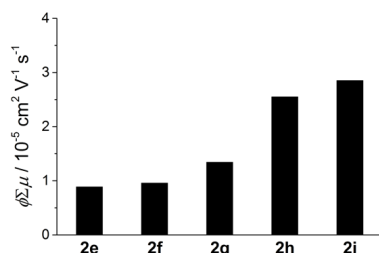

Figure 5. The maximum transient conductivities ($\phi\Sigma\mu$) of **2e**–**2i** observed upon excitation with a 355 nm laser pulse.

In summary, we have found that dissymmetrical substitution on *meso*-positions enables fine-tuning of properties of norcorroles with maintaining their stability. The optical and electrochemical properties of dissymmetrical norcorrole Ni^{II} complexes were considerably altered in comparison to dimesitylnorcorrole Ni^{II} complex by substituent effects. Furthermore, novel norcorroles showed various packing structures in crystal depending on the subtle structural change of aryl groups. The effect of packing structures on carrier mobilities of dissymmetric norcorroles was examined using TRMC technique. The conductivities correlated with the presence or absence of π–π stacking structures between norcorrole moieties. The present study has demonstrated that manipulation of *meso*-substituents of Ni^{II} norcorroles is effective to improve their low-energy absorption property as well as modulate their charge carrier mobility. These insights provided by the modification of norcorroles should promote further development of optical and electronic materials based on antiaromatic porphyrinoids.

Notes and references

1   (a) S. Miao, S. M. Brombosz, P. v. R. Schleyer, J. I. Wu, S. Barlow, S. R. Marder, K. I. Hardcastle and U. H. F. Bunz, *J. Am. Chem. Soc.*, 2008, **130**, 7339–7344; (b) M. Ishida, S.-J. Kim, C. Preihs, K. Ohkubo, J. M. Lim, B. S. Lee, J. S. Park, V. M. Lynch, V. V. Roznyatovskiy, T. Sarma, P. K. Panda, C.-H. Lee, S.

Fukuzumi, D. Kim and J. L. Sessler, *Nat. Chem.*, 2013, **5**, 15–20; (c) T. Satoh, M. Minoura, H. Nakano, K. Furukawa and Y. Matano, *Angew. Chem. Int. Ed.*, 2016, **55**, 2235–2238.

2   C. Fan, L. G. Mercier, W. E. Piers, H. M. Tuononen and M. Parvez, *J. Am. Chem. Soc.*, 2010, **132**, 9604–9606.

3   (a) D. T. Chase, A. G. Fix, S. J. Kang, B. D. Rose, C. D. Weber, Y. Zhong, L. N. Zakharov, M. C. Lonergan, C. Nuckolls and M. M. Haley, *J. Am. Chem. Soc.*, 2012, **134**, 10349–10352; (b) T. Nishinaga, T. Ohmae, K. Aita, M. Takase, M. Iyoda, T. Arai and Y. Kunugi, *Chem. Commun.*, 2013, **49**, 5354–5356; (c) L. Hu, N. Yan, Q. Chen, P. Zhang, H. Zhong, X. Zheng, Y. Li and X. Hu, *Chem. Eur. J.*, 2012, **18**, 8971–8977; (d) J. L. Marshall, K. Uchida, C. K. Frederickson, C. Schutt, A. M. Zeidell, K. P. Goetz, T. W. Finn, K. Jarolimek, L. N. Zakharov, C. Risko, R. Herges, O. D. Jurchescu and M. M. Haley, *Chem. Sci.*, 2016, **7**, 5547–5558; (e) B. Yuan, J. Zhuang, K. M. Kirmess, C. N. Bridgmohan, A. C. Whalley, L. Wang and K. N. Plunkett, *J. Org. Chem.*, 2016, **81**, 8312–8318; (f) T. Kawase, T. Fujiwara, C. Kitamura, A. Konishi, Y. Hirao, K. Matsumoto, H. Kurata, T. Kubo, S. Shinamura, H. Mori, E. Miyazaki and K. Takimiya, *Angew. Chem. Int. Ed.,* 2010, **49**, 7728–7732; (g) M. Nakano, I. Osaka, K. Takimiya and T. Koganezawa, *J. Mater. Chem. C,* 2014, **2**, 64-70

4   (a) H. Satoru and S. Hiroshi, in *Handbook of Porphyrin Science*, World Scientific Publishing, 2016, vol. 37, pp. 233–302. (b) J. Setsune, K. Kashihara, K. Wada and H. Shiozaki, *Chem. Lett.*, 1999, 847–848; (c) S. Mori and A. Osuka, *J. Am. Chem. Soc.*, 2005, **127**, 8030–8031; (d) M. Suzuki and A. Osuka, *J. Am. Chem. Soc.*, 2007, **129**, 464–465; (e) S. Shimizu and W. S. Cho, J. L. Sessler, H. Shinokubo, A. Osuka, *Chem. Eur. J.*, 2008, **14**, 2668–2678; (f) J. S. Reddy and V. G. Anand, *J. Am. Chem. Soc.*, 2008, **130**, 3718–3719; (g) Y. Yamamoto, Y. Hirata, M. Kodama, T. Yamaguchi, S. Matsukawa, K. Akiba, D. Hashizume, F. Iwasaki, A. Muranaka, M. Uchiyama, P. Chen, K. M. Kadish and N. Kobayashi, *J. Am. Chem. Soc.,* 2010, **132**, 12627–12638; (h) B. Szyszko, A. Białońska, L. Szterenberg and L. Latos-Grażyński, *Angew. Chem. Int. Ed.*, 2015, **54**, 4932–4936; (i) T. Furuyama, T. Sato and N. Kobayashi, *J. Am. Chem. Soc.*, 2015, **137**, 13788–13791; (j) B. K. Reddy, S. C. Gadekar and V. G. Anand, *Chem. Commun.*, 2016, **52**, 3007–3009; (k) A. Yamaji, H. Tsurugi, Y. Miyake, K. Mashima and H. Shinokubo, *Chem. Eur. J.*, 2016, **22**, 3956–3961.

5   M. Bröring, S. Kchler and C. Kleeberg, *Angew. Chem. Int. Ed.*, 2008, **47**, 5658–5660.

6   T. Ito, Y. Hayashi, S. Shimizu, J.-Y. Shin, N. Kobayashi and H. Shinokubo, *Angew. Chem. Int. Ed.*, 2012, **51**, 8542–8545.

7   (a) T. Fukuoka, K. Uchida, Y. M. Sung, J.-Y. Shin, S. Ishida, J. M. Lim, S. Hiroto, K. Furukawa, D. Kim, T. Iwamoto and H. Shinokubo, *Angew. Chem. Int. Ed.*, 2014, **53**, 1506–1509; (b) R. Nozawa, K. Yamamoto, J.-Y. Shin, S. Hiroto and H. Shinokubo, *Angew. Chem. Int. Ed.*, 2015, **54**, 8454–8457; (c) R. Nozawa, K. Yamamoto, I. Hisaki, J.-Y. Shin and H. Shinokubo, *Chem. Commun.*, 2016, **52**, 7106–7109; (d) R. Nozawa, H. Tanaka, W.-Y. Cha, Y. Hong, I. Hisaki, S. Shimizu, J.-Y. Shin, T. Kowalczyk, S. Irle, D. Kim and H. Shinokubo, *Nat. Commun.,* 2016, **7**, 13620 (doi: 10.1038/ncomms13620).

8   (a) B. Liu, X. Li, M. Stępień and P. J. Chmielewski, *Chem.Eur. J.*, 2015, **21**, 7790–7797; (b) Z. Deng, X. Li, M. Stępień and P. J. Chmielewski, *Chem. Eur. J.*, 2016, **22**, 4231–4246; (c) B. Liu, T. Yoshida, X. Li, M. Stępień, H. Shinokubo and P. J. Chmielewski, *Angew. Chem. Int. Ed.*, 2016, **55**, 13142–13146.

9   S. Seki, A. Saeki, T. Sakurai and D. Sakamaki, *Phys. Chem. Chem. Phys.*, 2014, **16**, 11093–11113.